Electronic Supplementary Material (ESI) for Journal of Materials Chemistry A.
This journal is © The Royal Society of Chemistry 2024

Supporting Information

A judicious hetero-dopants injection and abstraction of Co_3O_4 catalyst for efficient methane oxidation

Shiqiang Sun,[a,b,1] Guoling Li,[a,1] Shanhui Zhu,[c] Wenhao Meng,[a] Leilei Xu,[b] Jinlong Jiang,[d,*] Fagen Wang,[e] Xingyun Li[a,*]

[a]Institute of Materials for Energy and Environment, College of Materials Science and Engineering, Qingdao University, Qingdao 266071, China

[b]Collaborative Innovation Centre of the Atmospheric Environment and Equipment Technology, School of Environmental Science and Engineering, Nanjing University of Information Science & Technology, Jiangsu Key Laboratory of Atmospheric Environment Monitoring and Pollution Control, Joint International Research Laboratory of Climate and Environment Change (ILCEC), Nanjing 210044, China

[c]State Key Laboratory of Coal Conversion, Institute of Coal Chemistry, Chinese Academy of Sciences, Taiyuan 030001, China

[d]Key Laboratory for Palygorskite Science and Applied Technology of Jiangsu Province, National & Local Joint Engineering Research Center for Mineral Salt Deep Utilization, Faculty of Chemical Engineering, Huaiyin Institute of Technology, Huaian 223003, China

[e]School of Chemistry and Chemical Engineering, Jiangsu University, Zhenjiang 212013, China

Text S1 Catalysts characterizations

Field emission scanning electron microscope (SEM) and energy dispersion spectrometer (EDS) images were obtained on JEOL JSM-7800F, and transmission electron microscope (TEM) images were obtained on a JEOL JEM-2100. X-ray diffraction (XRD) pattern was recorded on a Rigaku Ultima IV with Cu-Kα radiation ($\lambda = 0.15418$). Inductively Coupled Plasma (ICP) was tested on Agilent ICP-OES/730. N_2 sorption experiment was performed on Quantachrome Autosorb iQ3 at 77 K. The specific surface area was calculated using the Brunauer-Emmett-Teller (BET) method, the pore size distribution was estimated with Density Functional Theory (DFT) method and X-ray photo-electron spectroscopy (XPS) was obtained on a PHI5000 Versaprobe III XPS spectrometer with an Al Ka X-ray source (1486.6 eV) and the in-depth XPS analysis were obtained by etching the surface with argon ions. Electron paramagnetic resonance (EPR) measurements were recorded on an FA-200 (JES) electron paramagnetic resonance spectrometer. Raman spectra were recorded on a Renishaw in Via Plus Micro-Raman spectroscopy system equipped with a 50 mW DPSS laser at 532 nm. H_2 temperature-programmed reduction (H_2-TPR) were estimated using a Quantachrome Chembet Pulsar analyzer. 30 mg of sample was pre-treated with Ar atmosphere at 200 ^{o}C for 30 min to remove the adsorbed volatiles, and then the sample was cooled to 50 ^{o}C. TPR curve was recorded with 5% hydrogen (balanced with Ar) at a flow rate of 100 mL·min^{-1} and a heating rate of 10 ^{o}C·min^{-1}. In-situ diffuse reflectance infrared Fourier transform spectroscopy (DRIFTs) was performed on a NICOLET iS50 infrared spectrometer (Thermo Fisher Scientific).

After the catalyst was deposited in the in-situ cell, 10 mL·min^{-1} of argon flow was introduced and maintained at 300 °C for 60 min, then the temperature was lowered from 300 °C to 50 °C. After background collection, the reaction feed containing 2 *vol.*% CH_4, 20 *vol.*% O_2 and is balanced with Ar was additionally introduced into the cell with the temperature gradually raised to 450 °C. In the meantime, IR spectra acquisition was conducted under 50 °C, 150 °C, 250 °C, 350 °C and 450 °C after the temperature stabilization.

Text S2 Density functional theory (DFT) calculation method

The plane-wave-based periodic DFT method was carried out with the Vienna *ab initio* simulation package (VASP).[1,2] The projector augmented wave (PAW) setups was used to describe the electron-ion interactions, while the exchange and correlation energy were selected to be parameterized by the Perdew, Burke and Engerhoff (PBE) functional.[3,4] Based on XRD and TEM results, the Co_3O_4 (311) was modeled using a four-layer periodic slabs. Cr doped Co_3O_4 (311) facet was modeled with three Co atoms substituted by three Cr atoms, which was designated as Cr-Co_3O_4 (311). The Cr doped Co_3O_4 (311) facet with Cr vacancy was built by removing one surface Cr atoms, which was named as Cr-Co_3O_4-OH (311). The oxygen vacancy formation energy (E (O_v)) on different models were defined by the following formulas:

$$E\,(O_v) = E(\text{Cr-}Co_3O_{4-x}) + 1/2E(O_2) - E(\text{Cr-}Co_3O_4)$$

Where E(Cr-Co_3O_{4-x}) represents the energy of Cr doped Co_3O_4 (311) slab model with oxygen vacancy (surface oxygen vacancy was created by removing one O atom.), $E(O_2)$ corresponds to the energy of O_2 gas molecule, and E(Cr-Co_3O_4) is the energy of

Cr doped Co_3O_4 slab model.

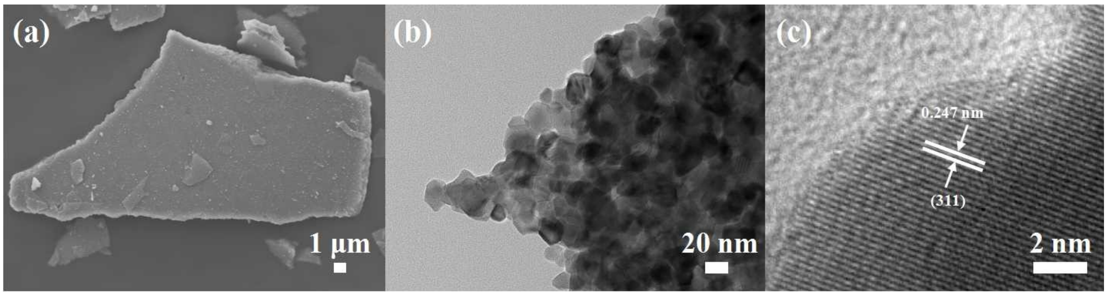

Fig. S1 (a) SEM, (b) TEM and (c) HR-TEM image of Co_3O_4.

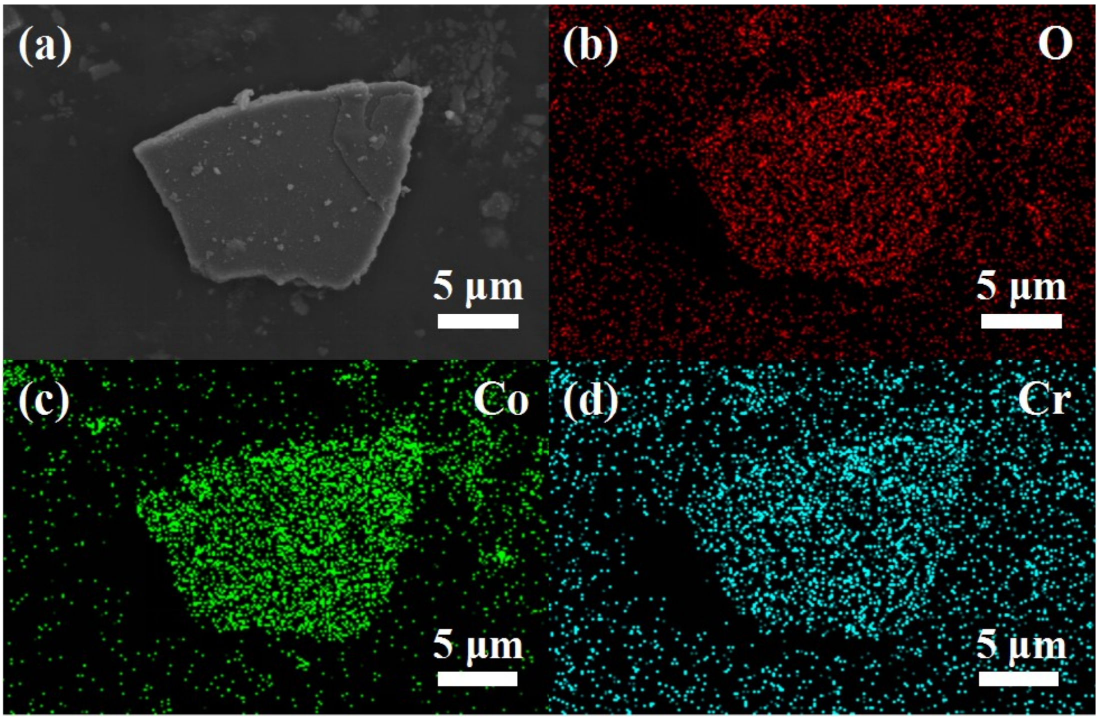

Fig. S2 (a) SEM image, and EDS elemental mapping of (b) O, (c) Co and (d) Cr for Cr-Co_3O_4.

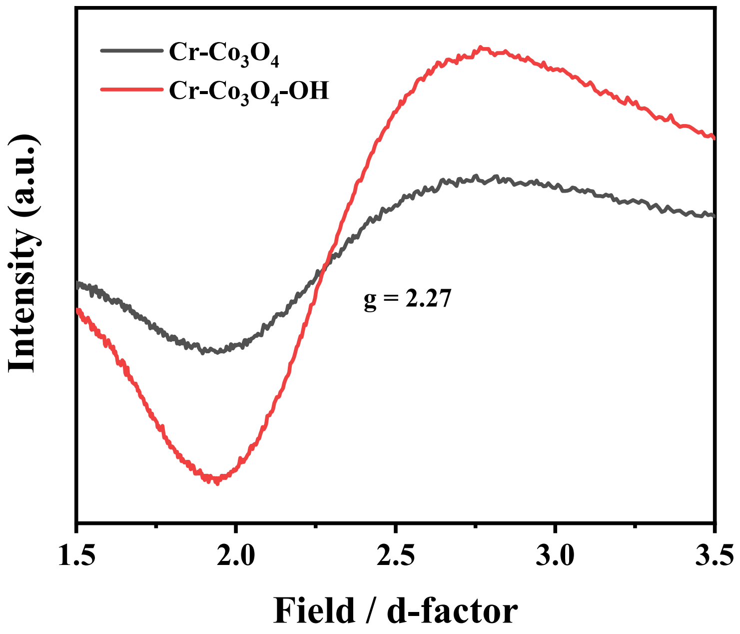

Fig.S3 EPR spectra for Cr-Co_3O_4 and Cr-Co_3O_4-OH.

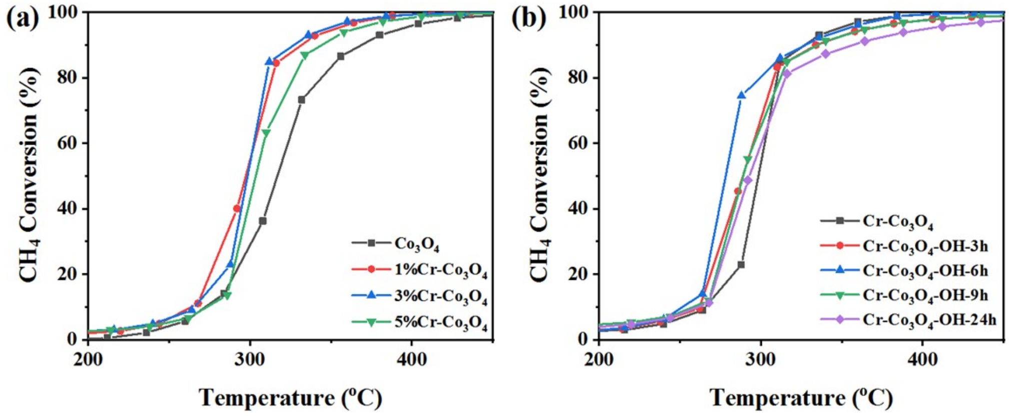

Fig. S4 CH_4 oxidation performances (reaction condition: 2 *vol.*% of CH_4, 20 *vol.*% O_2, Ar as balance gas, flow velocity = 66 mL·min^{-1}, WHSV = 40,000 mL·g^{-1}·h^{-1}) of (a) Co_3O_4 with different Cr doping amounts and (b) Cr-Co_3O_4 that etched in alkali for different time.

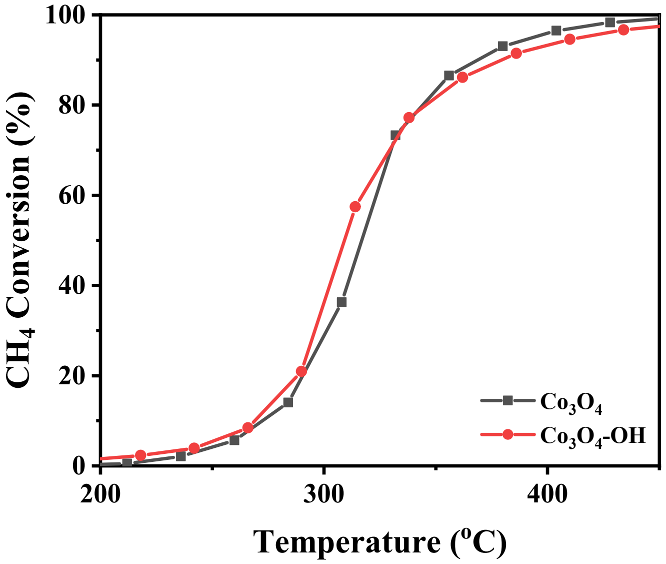

Fig. S5 CH_4 oxidation performances (reaction condition: 2 *vol.*% of CH_4, 20 *vol.*% O_2, Ar as balance gas, flow velocity = 66 mL·min^{-1}, WHSV = 40,000 mL·g^{-1}·h^{-1}) of Co_3O_4 and Co_3O_4-OH.

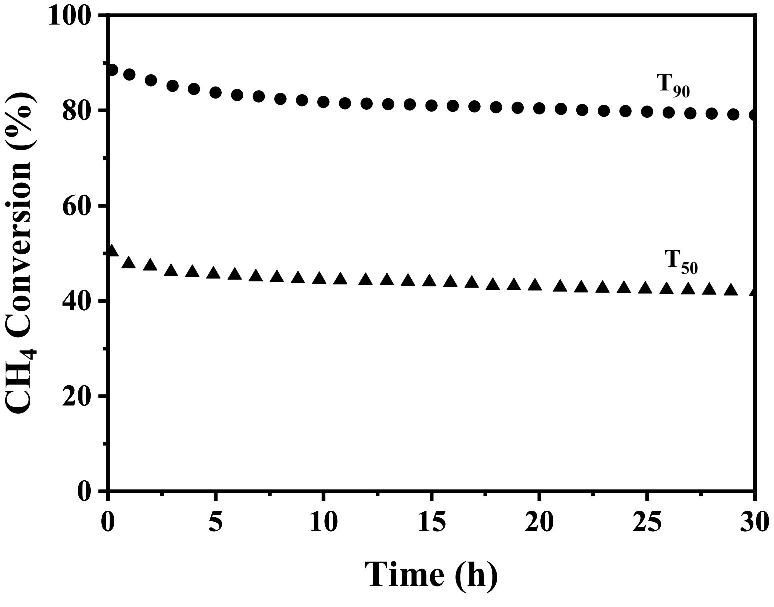

Fig. S6 Stability test of Cr-Co_3O_4-OH at reaction temperature of T_{90} (327 °C) and T_{50} (278 °C) (reaction condition: 2 *vol.*% of CH_4, 20 *vol.*% O_2, Ar as balance gas, flow velocity = 66 mL·min^{-1}, WHSV = 40,000 mL·g^{-1}·h^{-1}).

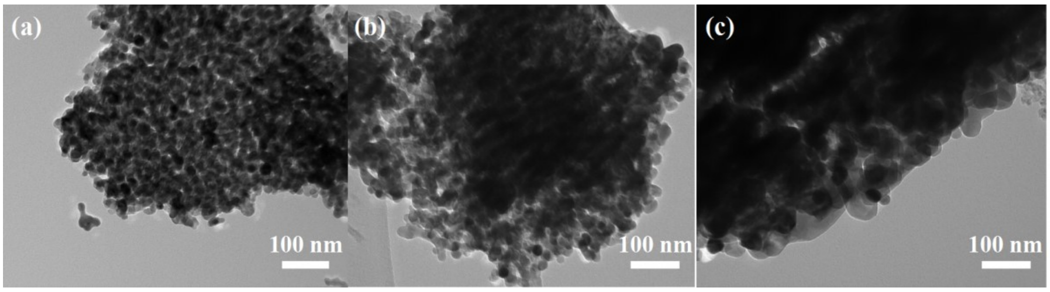

Fig. S7 TEM images of Cr-Co_3O_4-OH, Cr-Co_3O_4-OH-T_{50} and Cr-Co_3O_4-OH-T_{90}.

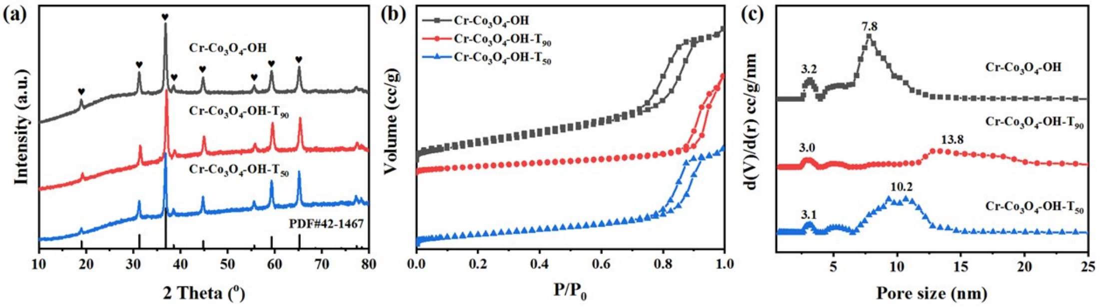

Fig. S8 (a) XRD patterns, (b) N_2 sorption isotherm and (c) NL-DFT pore size distribution for the catalysts of Cr-Co_3O_4-OH, Cr-Co_3O_4-OH-T_{50} and Cr-Co_3O_4-OH-T_{90}.

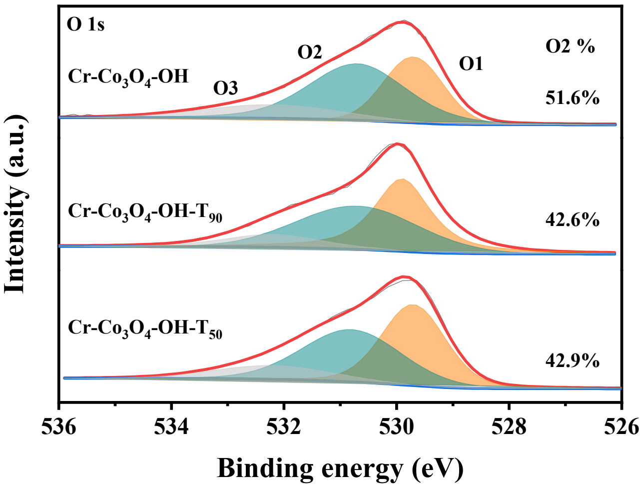

Fig. S9 O 1s XPS spectra for Cr-Co_3O_4-OH, Cr-Co_3O_4-OH-T_{50} and Cr-Co_3O_4-OH-T_{90}.

Table S1 Cr content of Cr-Co_3O_4 at different Ar ions etching time by XPS.

location	etching time

	0 min	10 min
1	4.06 *wt.*%	2.05 *wt.*%
2	4.24 *wt.*%	2.16 *wt.*%
3	4.56 *wt.*%	1.94 *wt.*%

Table S2 Cr content of Cr-Co_3O_4-OH at different Ar ions etching time by XPS.

location	etching time	
	0 min	10 min
1	2.63 *wt.*%	2.09 *wt.*%
2	2.49 *wt.*%	2.04 *wt.*%
3	2.13 *wt.*%	2.15 *wt.*%

Table S3 Crystallite size, specific surface area and surface information of the catalysts.

Sample	Crystallite size [a] (nm)	Specific surface area [b] ($m^2 \cdot g^{-1}$)	O_v (%) [c]
Cr-Co_3O_4-OH	18.2	67.4	51.6
Cr-Co_3O_4-OH-T_{90}	21.9	23.5	42.6
Cr-Co_3O_4-OH-T_{50}	18.7	37.4	42.9

[a] Crystallite size calculated by Scherrer formula.

[b] Pore volume calculated at P/P_0 of 0.99.

[c] Data determined from XPS results.

References

1 G. Kresse, *J. Hafner, Phys. Rev. B.*, 1993, **47**, 558-561.

2 G. Kresse, J. Furthmüller, *Comp. Mater. Sci.*, 1996, **6**, 15-50.

3 G. Kresse, D. Joubert, *Phys. Rev. B.*, 1999, **59**, 1758-1775.

4 P. E. Blöchl, *Phys. Rev. B.*, 1994, **50**, 17953-17979.